Laser-induced singlet oxygen selectively triggers oscillatory mitochondrial permeability transition and apoptosis in melanoma cell lines

Running title Singlet oxygen induces apoptosis in melanoma

Irina N. Novikova[a,*], Elena V. Potapova[a,*], Viktor V. Dremin[a,b], Andrey V. Dunaev[a], Andrey Y. Abramov[a,c]

[a] Cell Physiology and Pathology Laboratory, Orel State University, Orel, Russia

[b] College of Engineering and Physical Sciences, Aston University, Birmingham, UK

[c] Department of Clinical and Movement Neurosciences, UCL Queen Square Institute of Neurology, London, UK

*These authors contributed equally to this work

Corresponding authors: Prof Andrey Y. Abramov a.abramov@ucl.ac.uk

Dr Irina N. Novikova irina.makovik@gmail.com

Abstract

Singlet oxygen ($^1O_2$) is an electronically excited state of triplet oxygen which is less stable than molecular oxygen in the electronic ground state and produced by photochemical, thermal, chemical, or enzymatic activation of O_2. Although the role of singlet oxygen in biology and medicine was intensively studied with photosensitisers, using of these compounds is limited due to toxicity and lack of selectivity. We generated singlet oxygen in the skin fibroblasts and melanoma cell lines by 1267 nm laser irradiation. It did not induce production of superoxide anion, hydrogen peroxide or activation of lipid peroxidation in these cells confirming high selectivity of 1267 nm laser to singlet oxygen. $^1O_2$ did not change mitochondrial membrane potential ($\Delta\Psi m$) in skin fibroblasts but induced fluctuation in $\Delta\Psi m$ and complete mitochondrial depolarisation due to opening permeability transition pore in B16 melanoma cells. 1267 nm irradiation did not change the percentage of fibroblasts with necrosis but significantly increased the number of B16 melanoma cells with apoptosis. Thus, singlet oxygen can induce apoptosis in cancer B16 melanoma cells by opening of mitochondrial permeability transition pore (PTP) but not in control fibroblasts.

***Abbreviations*:** $^1O_2$, singlet oxygen; $\Delta\Psi m$, Mitochondrial membrane potential; PTP, mitochondrial Permeability Transition Pore; ROS, reactive oxygen species; SOSG, Singlet Oxygen Sensor Green; DHE, dihydroethidium; DCFH-DA, 2′,7′-dichlorodihydrofluorescein diacetate; MCB, monochlorobimane; TMRM, Tetramethylrhodamine; GSH, glutathione; NucView 488, NucView™ 488 Caspase-3 Substrate.

1. INTRODUCTION

Biological tissues require oxygen for normal functioning of energy metabolism. High biological and chemical activity of oxygen is caused by high redox potential that enables it to accept electrons easily from reduced substrates. Different forms of reactive oxygen species (ROS; radical and non-radical) have even higher activity, produced in cells in enzymatic and non-enzymatic way and are

used in redox signalling and many cellular processes: cell proliferation, survival, migration, differentiation, programmed cell death, organogenesis, though ROS overproduction may lead to oxidative stress [1–3].

Various reactive forms of oxygen play role in physiological process and redox biology but longer living hydrogen peroxide and singlet oxygen could be more involved in signalling processes [4–7]. $^1O_2$ is an electronically excited state of triplet oxygen which is less stable than molecular oxygen in the electronic ground state. Singlet oxygen is produced by photochemical, thermal, chemical, or enzymatic activation of O_2 and used as an effector of gene expression and regulator of mitochondrial bioenergetics [8–10].

$^1O_2$ interacts with various compounds and produces endoperoxides that may lead to forming of radicals and other forms of ROS, aldehydes etc. Considering high biological activity and the ability to initiate oxidative stress-induced cell death, induction of singlet oxygen in photodynamic therapy was intensively studied for development of strategy of cell death induction in tumours [11,12].

A wide range of photosensitizers had been used for $^1O_2$ production in biological tissues [13]. However, the application of of the photosensitizers is limited by their toxicity and non-selectivity for singlet oxygen. During the last decade, it was shown that $^1O_2$ can be produced without any chemical compounds by specific wavelengths excitation [14,15]. Oxygen has the highest adsorption coefficient at 1262-1268 nm and considering this lasers with ~1270 nm are now intensively used for generation of singlet oxygen in different tissues [12,16–18]. However, 1265 nm laser-induced singlet oxygen led to free radicals production, mitochondrial dysfunction and cell death in cancer and cell cultures [12,18]. In contrast singlet oxygen had no toxic effect in primary astrocytes and neurons and it activated mitochondrial bioenergetics [10]. Considering this, we suggested that singlet oxygen may have different effect on the viability of cells from different tissues. Here, we studied the effect of 1267 nm laser-induced singlet oxygen on ROS production, oxidative stress, and cell viability of cancer B16 melanoma cells compared to control fibroblasts. We have found that 1267 nm irradiation produced singlet oxygen but not superoxide anion or hydrogen peroxide and did not induce oxidative

stress in both B16 melanoma cells and fibroblasts. The cells exposure to 1267 nm laser induced opening of the mitochondrial permeability transition pore and apoptosis in B16 melanoma cells but not in fibroblasts suggesting higher vulnerability of the melanoma cells to singlet oxygen compared to control fibroblasts.

2. Methods

Cell culture

Control human skin fibroblasts [19] and melanoma cell line B16 were used as a research object. B16 cells were cultured in the DMEM (Gibco, Paisley, UK), 10% FBS (Biological Industries, Kibbutz Beit-Haemek, Israel), penicillin (100 U/ml), streptomycin (100 μg/ml) (Gibco, New York, USA). DMEM (Biological Industries, Kibbutz Beit-Haemek, Israel), 10% FBS (Biological Industries, Kibbutz Beit-Haemek, Israel) with 1% GlutaMAX (Gibco, New York, USA) were applied for cultivation of skin fibroblasts. Cell cultures were maintained at 37 °C in a humidified atmosphere of 5% CO_2 and 95% air. The confluence of cells during the studies was 40-50%.

Laser specification

Laser diodes LD-1267-PM-500 and LD-1122-PM-500 (Innolume GmbH, Dortmund, Germany) were used as sources of laser radiation at wavelengths 1267 and 1122 nm. Laser diode driver SF8150-ZIF14 (Maiman Electronics LLC, Saint-Petersburg, Russia) and Maiman Benchsoft software were applied to power and control laser diodes.

Laser radiation from the source to the study object was carried out using a specially manufactured quartz fiber-optic cable. The cable provided radiation transmission with minimal signal attenuation in the spectral range of 400-2000 nm and numeric aperture NA=0.22±0.02. Collimator F280FC-C (Thorlabs Inc., Mölndal, Sweden) was installed to form a parallel beam of laser radiation after a fiber-optic cable that enabled the stability of the experimental studies. Collimator eliminated dependence

of laser radiation dose from the distance "end of the fiber-optic cable - the object of the study" with a divergent light beam. The diameter of the laser radiation beam at the collimator output was 3.4 mm.

Live cell imaging

Fluorescence measurements were obtained using confocal microscope LSM 900 with Airyscan 2 (Carl Zeiss Microscopy GmbH, Jena, Germany). Illumination intensity was kept to a minimum (0.1-0.2% of laser output) to avoid phototoxicity.

Singlet oxygen production

Mitochondrial singlet oxygen production was measured using 10 μM Singlet Oxygen Sensor Green (SOSG, Invitrogen, Oregon, USA) (excitation 488 nm laser with emission 525 nm) without application of photosensitiser.

ROS production

Superoxide production was measured by using 5 μM dihydroethidium (DHE, Invitrogen Oregon, USA) (excitation 405 nm with emission at 460 nm).

To detect intracellular ROS (mostly hydrogen peroxide), 2′,7′-dichlorodihydrofluorescein diacetate (DCFH-DA, Cayman Chemical Co., Michigan, USA) (excitation/emission maxima ~492-495/517-527 nm) was used at 20 μM.

MitoTracker Red CM-H_2Xros (Invitrogen, Oregon, USA) (excitation 530 nm laser with emission above 580nm) in concentration 1 μM was used for analysis of ROS production in mitochondria.

No preincubation (“loading”) was used for these fluorescence probes to avoid the intracellular accumulation of oxidized probe.

Lipid peroxidation and GSH level

The rate of lipid peroxidation was measured using 10 μM LiperFluo (Dojindo Molecular Technologies Inc., Kumamoto, Japan) (excitation/emission maxima ~500/590 nm).

To measure the intracellular glutathione, the glutathione-sensitive fluorescent probe monochlorobimane (MCB, Invitrogen, Oregon, USA) (excitation/emission maxima ~380/461 nm) was used. Cells were pre-treated with a laser 1267 nm or 1122 nm followed by 20 min incubation. After that cells were loaded with 50 μM MCB for 30 min at 37 °C.

Measurement of the mitochondrial membrane potential (ΔΨm)

Cells were incubated with 25 nM Tetramethylrhodamine (TMRM, Invitrogen, Oregon, USA) (excitation 530 nm laser, emission above 574 nm) for 30 min at 37°C. Measurements of ΔΨm were performed in a single focal plane during the fixed time period. The protonophore FCCP (Sigma-Aldrich, Missouri, USA) (1 μM) was added at the end of each experiment.

Cyclosporine A was used as an inhibitor of mitochondrial permeability transition (PTP). Cells were pre-incubated with 1 μM cyclosporine A in a Hanks balanced salt solution (HBSS) for 20 min at 37°C.

Cell death

The measurement of necrotic cells death was carried out using Hoechst 33342 and Propidium Iodide. Cells were incubated with 5 μM Hoechst 33342 (Invitrogen, Oregon, USA) (excitation/emission maxima ~350/481 nm) and 20 μM Propidium iodide (Invitrogen, Oregon, USA) (excitation/emission maxima ~535/617 nm) for 30 min at 37°C.

NucView™ 488 Caspase-3 Substrate (NucView 488, Biotium, California, USA) (excitation laser 488 nm with emission above 515 nm) in combination with Hoechst 33342 was applied for detection of caspase-3/7 activation and visualization of morphological changes in the nucleus during apoptosis. Cells were incubated with 5 μM NucView 488 and 5 μM Hoechst 33342 for 30 min at the room

temperature. For all experiments we kept the same experimental setting to avoid misinterpretation of results.

Cell death was measured 24 hours after treatment of cells with lasers.

Data analysis and statistics

Data and statistical analyses were performed using OriginPro (OriginLab Corp., Northampton, USA) software. Data are presented as means expressed ± standard error of the mean (SEM). Differences were considered to be significantly different if $p < 0.05$ by ANOVA with the Tukey post hoc test.

RESULTS

Singlet oxygen production by 1267 nm laser illumination in fibroblasts and B16 cells

We used SOSG as fluorescent indicator for singlet oxygen to study the effect of 1267 nm laser irradiation on generation of this reactive form of oxygen in skin fibroblasts and melanoma cell lines B16. We found that both cell types have a similar basal level of singlet oxygen generation (Figure 1A-D). However, illumination of these cells with 1267 nm laser (200 J/cm^2) induced fast and profound increase in the rate of singlet oxygen production in both B16 line and fibroblasts (N=3, n=16 cells of B16 upon 1267 nm, n=20 cells of B16 upon 1122 nm and n=11 cells of fibroblasts upon 1267 nm; n=8 cells of fibroblasts upon 1122 nm; Figure 1A-D). It should be noted that control laser line 1122 nm did not change the rate of singlet oxygen production in B16 cells and fibroblasts (Figure 1A-D). Considering the effect of singlet oxygen on specific organelles, we have tested the distribution of the SOSG fluorescence in the cells before and after treatment with 1267 nm laser. Lateral and transversal profiles of SOSG in B16 melanoma cells show uneven distribution of the fluorescence before and after treatment with 1267nm laser (Figure 1 Ei-iii; Fi-iii). Although potentially specific probes for detection of various organelles could be used, the distribution of the SOSG fluorescence is not efficient enough to make conclusion about any specific localisation of singlet oxygen inside

the cells. Thus, 1267 nm laser induced singlet oxygen generation in cancer cell line B16 and control fibroblasts.

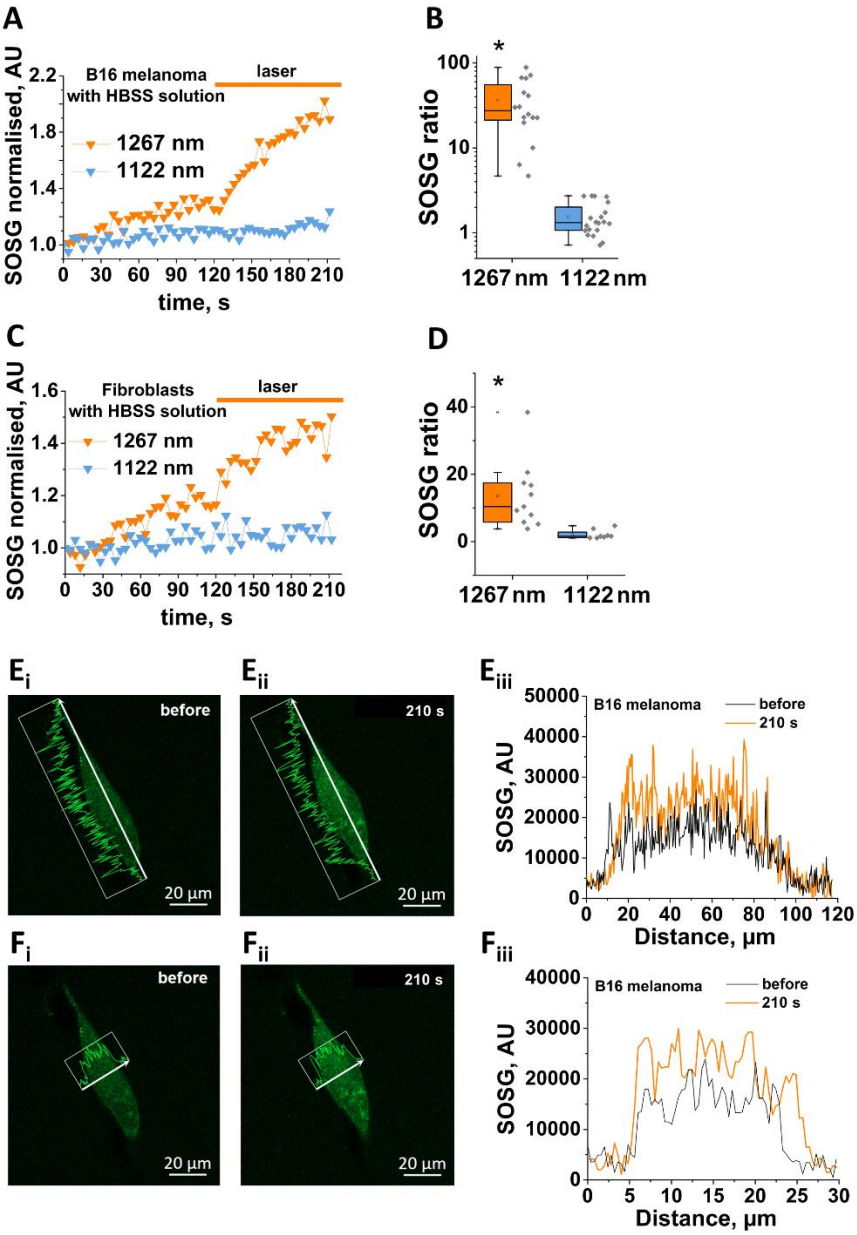

Fig. 1. Singlet oxygen production by 1267 nm laser illumination

Representative normalized traces of the effect of 200 J/cm^2 dose induced by 1122 nm and 1267 nm illumination on the SOSG fluorescence in the melanoma cell line B16 (A) and in the skin fibroblasts (C). The rates of singlet oxygen production for 1122 nm and 1267 nm illumination in the B16 melanoma (B) and in the skin fibroblasts (D). Ei-iii, Fi-iii Profiles of the SOSG fluorescence in B16 melanoma cells before and after 200 J/cm^2 dose induced by 1267 nm laser *$p < 0.05$.

1267 nm laser has no effect on production of other forms of ROS in B16 cells

Previously, it was shown that 1267 nm laser irradiation is capable of triggering prolonged cellular oxidative stress by the impulse perturbation of redox homeostasis in cancer cells which is induced by production of various forms of ROS [12].

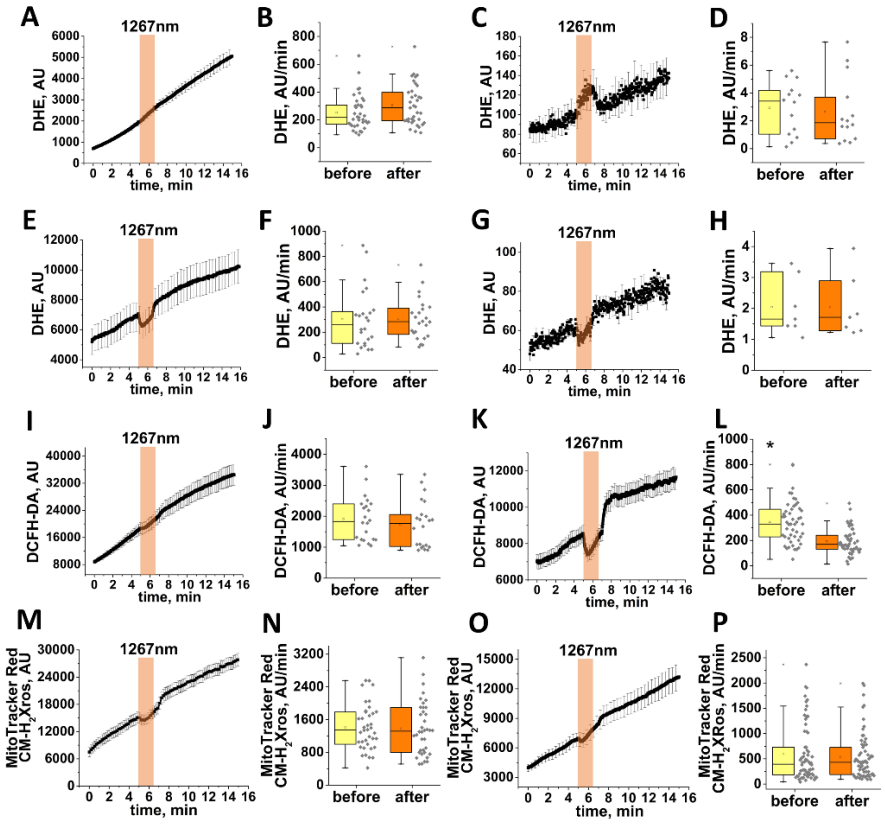

Fig. 2. 1267 nm laser has no effect on production of other forms of ROS

Average traces of the DHE fluorescence in the melanoma cell line B16 (A), in the skin fibroblasts (E) and the extracellular of DHE fluorescence for each group (C, G) upon 1267 nm illumination. The rates of superoxide production in the melanoma cell line B16 (B), in the skin fibroblasts (F) and the extracellular of DHE fluorescence for each group (D, H) before and after 1267 nm illumination. Average traces of the DCFH-DA fluorescence in the melanoma cell line B16 (I) and in the skin fibroblasts (K) upon 1267 nm illumination. The rates of superoxide production in the melanoma cell line B16 (J), in the skin fibroblasts (L) before and after 1267 nm illumination. Average traces of the MitoTracker Red CM-H2Xros fluorescence in the melanoma cell line B16 (M) and in the skin fibroblasts (O) upon 1267 nm illumination. The rates of superoxide production in the melanoma cell line B16 (N), in the skin fibroblasts (P) before and after 1267 nm illumination. *$p < 0.05$.

Considering this we have tested if 1267 nm laser irradiation can directly or indirectly (through activation of enzymatic ROS production) induce other forms of ROS. Although DHE can be oxidised by various ROS, it is mainly sensitive to superoxide anion [20,21]. Illumination of B16 melanoma cells (N=3 experiments, n=38 cells; Figure 2A-D) or skin fibroblasts (N=3 experiments, n=24 cells; Figure 2E-H) with 1267 nm laser (200 J/cm^2) did not change the rate of DHE oxidation in both cell types that strongly suggests that 1267 nm laser has no effect on superoxide production in both cell types. DCFH-DA, as well as other fluorescent indicators for ROS, can detect a number of ROS but it is shown to be more selective for hydrogen peroxide [22]. Laser 1267 nm (200 J/cm^2) had no effect on the rate of DCFH-DA oxidation or even decrease it in both skin fibroblasts and B16 melanoma cells (N=3 experiments for each type of cells, n=23 cells for fibroblasts, n=49 B16 cells; Figure 2I-L). Thus, 1267 nm laser has no effect on the hydrogen peroxide production in cells.

1267 nm laser has no effect on mitochondrial ROS production in fibroblasts and B16 cells

1267 nm laser-induced singlet oxygen activates mitochondrial metabolism [10]. Mitochondrial ROS production is dependent on the number of parameters including metabolic state [23]. Considering this, 1267 nm laser can potentially induce changes in mitochondrial ROS production. However, 1267 nm laser or control laser 1122 nm (200 J/cm^2) did not change the rate of ROS production in B16 cells or skin fibroblasts, measured by MitoTracker Red CM-H_2Xros (N=3, n=38 cells of B16, n=66 cells of fibroblasts; Figure 2M-P). Thus, 1267 nm laser at the dose 200 J/cm^2 selectively produces only singlet oxygen that does not change enzymatic ROS production in fibroblasts and melanoma cells.

1267 nm-induced singlet oxygen has no effect on lipid peroxidation and GSH level in fibroblasts and B16 cells

Changes in the redox balance caused by ROS overproduction or changes in antioxidant biosynthesis lead to oxidative stress and damage of biomolecules. Although 1267 nm laser had no

effect on the production of superoxide and hydrogen peroxide in our experiments, overproduction of singlet oxygen also shown to be able to induce oxidative stress [24]. Lipid peroxidation is involved in signalling process [25], however, products of lipid peroxidation are widely accepted to be a hallmark of oxidative stress [26]. Production of singlet oxygen by 1267 nm illumination (200 J/cm^2) had no effect on the rate of lipid peroxidation or even decreased it in fibroblasts (N=3, n=18 cells; Figure 3A-B) or B16 melanoma cells (N=3, n=29 cells; Figure 3C-D).

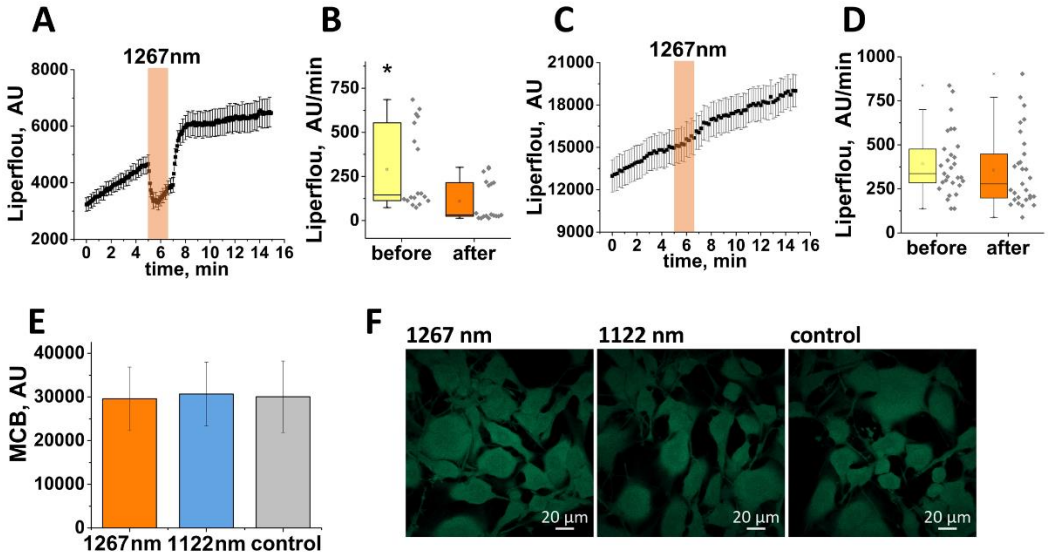

Fig. 3. 1267 nm-induced singlet oxygen has no effect on lipid peroxidation and GSH level

Average traces of the LiperFluo fluorescence in the skin fibroblasts (A) and in the melanoma cell line B16 (C) upon 1267 nm illumination. The rates of lipid peroxidation in the skin fibroblasts (B) in the melanoma cell line B16 (D) before and after 1267 nm illumination.

GSH level in the melanoma cell line B16 (E) upon 1267 nm illumination, 1122 nm illumination and control cells. Representative confocal images of MCB from the melanoma cell line B16 (F) upon 1267 nm illumination, 1122 nm illumination and control cells.

The level of major endogenous antioxidant GSH is sensitive to redox changes and immediately reflects oxidative stress. Measurements of GSH level with MCB in B16 melanoma cells treated with 1267 nm laser show that singlet oxygen at this dose of illumination (200 J/cm^2) had no effect on the level of this antioxidant in this type of cells (N=3, B16: n=436 cells upon 1267 nm, n=426 cells upon

1122 nm and n=418 control cells; Figure 3E-F). Thus, 1267 nm-induced singlet oxygen does not induce oxidative stress in cells.

Laser-induced $^1O_2$ production induces PTP opening in B16 cells but not in control fibroblasts

ΔΨm is maintained by function of electron transport chain of mitochondria with a number of rescuing mechanisms (such a reverse mode of F0-F1-ATPase) due to high importance of ΔΨm for mitochondria and cell life[27]. In agreement with previously published [10], 1267 nm illumination (200 J/cm^2) of skin fibroblasts induced mild (~10-15%) mitochondrial hyperpolarisation (Figure 4A), while control laser 1122 nm had no effect on ΔΨm (Figure 4B). Illumination of B16 cells with control 1122 nm laser also had no effect on mitochondrial membrane potential (Figure 4C). However, singlet oxygen induced by 200 J/cm^2 1267nm in B16 melanoma cells induced fast and transient changes in TMRM fluorescence (Figure 4D). Importantly, the shapes of ΔΨm changes were different – from fast and complete loss of membrane potential (Figure 4E, F) to the oscillations in TMRM signal (Figure 4G) (Figure 4H). Application of protonophore FCCP (1 μM) in the end of experiments clearly indicated complete loss of ΔΨm in majority of mitochondria (Figure 4A-D). Pre-incubation (20 min) of the B16 melanoma cells with inhibitor of PTP – 1 μM cyclosporine A not only prevented singlet oxygen- induced loss ΔΨm of any shapes but also led to increase in TMRM fluorescence (Figure 4I) similar to observed in neurons and astrocytes [10] and in fibroblasts. Thus, 1267 nm laser-induced singlet oxygen induces specific PTP opening for B16 melanoma cells but not for other type of cells.

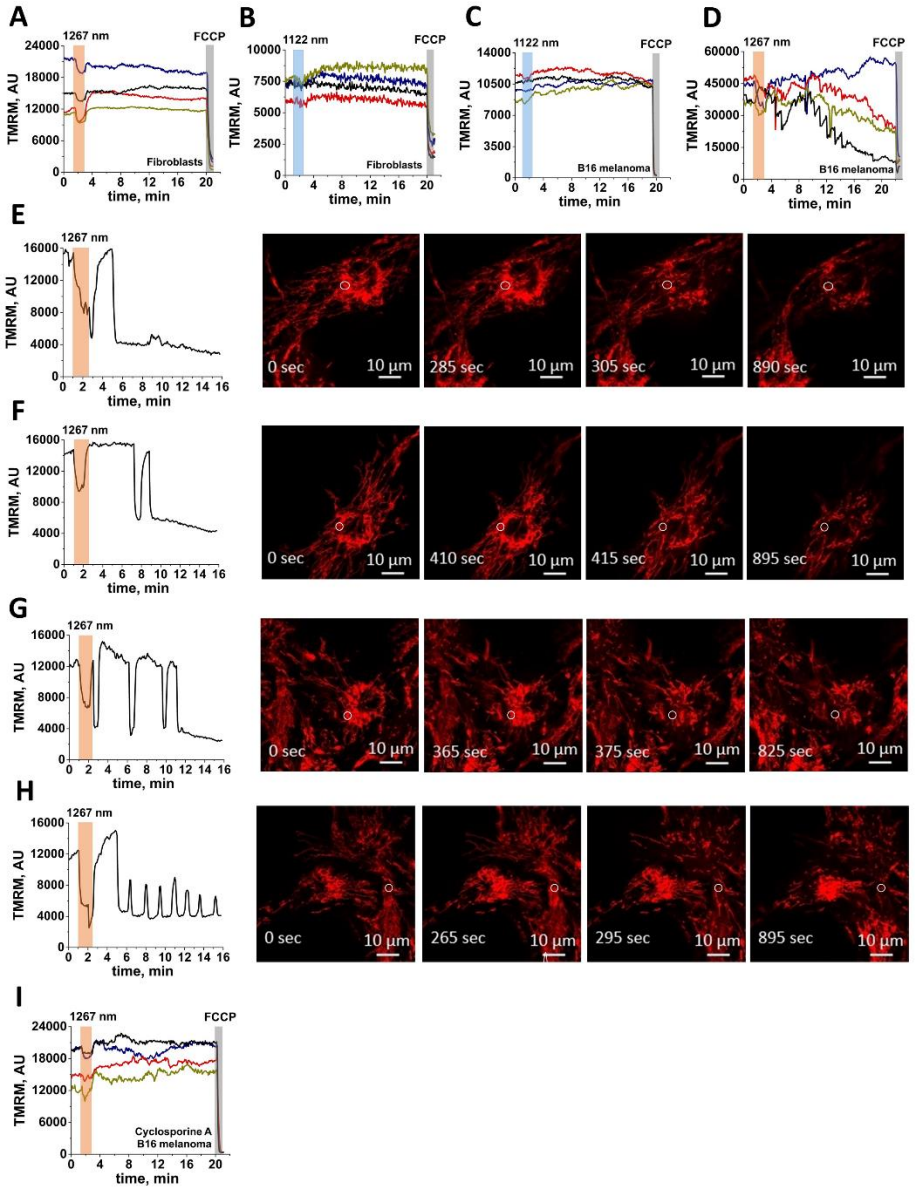

Fig. 4. Influence of laser-induced $^1O_2$ production on mitochondrial membrane potential

Representative traces of changes in mitochondrial membrane potential of the skin fibroblasts upon 1267 nm illumination (A), upon 1122 nm illumination (B) and the melanoma cell line B16 upon 1122 nm illumination (C), upon 1267 nm illumination (D) measured as intensity of TMRM fluorescence. Representative traces and confocal images of the different shapes of mitochondrial membrane potential changes: the fast and complete loss of TMRM fluorescence (E, F), the oscillations in mitochondrial membrane potential (G) and combinations of these changes (H). Representative traces of changes in mitochondrial membrane potential of the melanoma cell line B16 upon 1267 nm illumination after pre-incubation with inhibitor of mitochondrial permeability transition pore cyclosporine A (I).

1267 nm laser-induced singlet oxygen induces apoptosis but not necrosis in B16 melanoma

PTP opening is involved in the mechanism of necrosis and apoptosis [28]. Treatment of fibroblasts or B16 cells with 1267 nm (200 J/cm^2) or with singlet oxygen-free 1122 nm (200 J/cm^2) did not change the percentage of Propidium iodide – labelled cells in all studied groups (Figure 5A-D) that strongly suggests that singlet oxygen in this concentration has no effect on the necrosis in both fibroblasts and B16 melanoma cells (fibroblasts: 0% of cells (necrotic cells – 0, total number of cells – 472) upon 1267 nm and <1% of control cells (necrotic cells – 1, total number of cells – 453); B16: <1% of cells (necrotic cells – 8, total number of cells – 1209) upon 1267 nm, ~1% of cells (necrotic cells – 12, total number of cells – 953) upon 1122 nm and <1% of control cells (necrotic cells – 3, total number of cells – 1221); Figure 5B, D). However, in 1267 nm laser-treated B16 cells Hoechst labelled nuclei of the cells changed the shape to typical for apoptosis the morphological fragmentation of nuclei (fibroblasts: <1% of cells (apoptotic cells – 4, total number of cells – 472) upon 1267 nm and ~1% of control cells (apoptotic cells – 5, total number of cells – 453); B16: 7.6% of cells (apoptotic cells – 92, total number of cells – 1209) upon 1267 nm, 2.8% of cells (apoptotic cells – 27, total number of cells – 953) upon 1122 nm and ~2% of control cells (apoptotic cells – 27, total number of cells – 1221); Figure 5E) that suggests activation of apoptosis in these cells by singlet oxygen and PTP opening. To prove it we used NucView 488 – which become fluorescent after activation of caspase 3 [29]. Control laser 1122 nm did not induce changes in a number of NucView 488-labelled nucleus in B16 melanoma cells (5% of cells (apoptotic cells – 691, total number of cells – 13885); Figure 5F,G) while 1267 nm laser irradiation activates apoptosis in most of the B16 melanoma cells (47% of cells (apoptotic cells – 5448, total number of cells – 11764); Figure 5F,G), but not in fibroblasts (<1% of cells (apoptotic cells – 3, total number of cells – 954); Figure 5H,I).

Although two different methods shown different percentage of the melanoma cells with apoptosis (7.6% and 47%) that can be explained by methodological problems or by difference between actual apoptosis and caspase 3 activation these data clearly indicating that 1267 nm laser-induced apoptosis but not necrosis selectively in B16 melanoma cells but not in control fibroblasts.

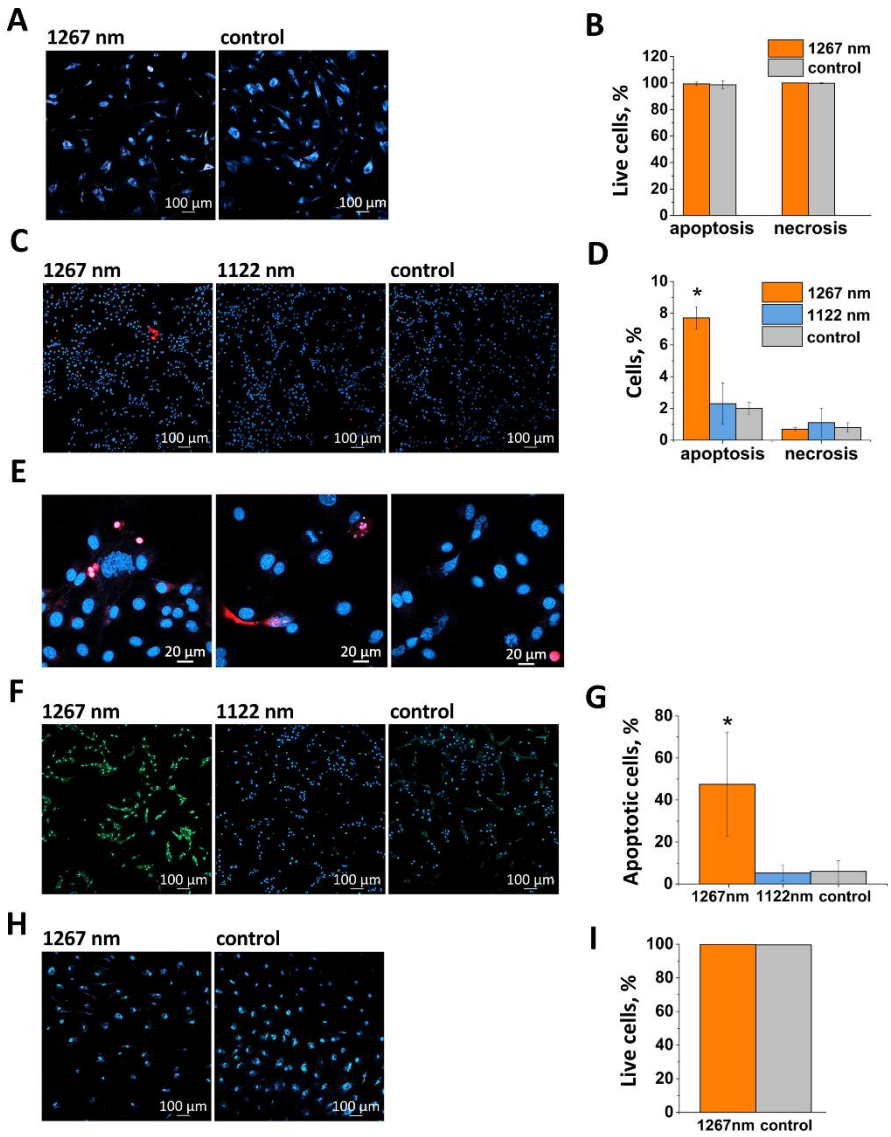

313

314 **Fig. 5. 1267 nm laser-induced singlet oxygen induces apoptosis but not necrosis in B16**
315 **melanoma and not in fibroblasts**

316 Representative confocal images of fibroblasts upon 1267 nm illumination and control fibroblasts by
317 using Propidium Iodide and Hoechst 33342 (A). Results of statistical processing of fibroblasts cell
318 death (N=4 (472 cells) for 1267 nm, N=4 (453 cells) for control cells) (B). Representative confocal
319 images of the melanoma cell line B16 upon 1267 nm illumination, upon 1122 nm illumination and
320 control cells by using Propidium Iodide and Hoechst 33342 (C). Results of statistical processing of
321 cell death (N=2 (1209 cells) for 1267 nm, N=3 (953 cells) for 1122 nm, N=3 (1221 cells) for control
322 cells) (D). Representative confocal images of apoptosis fragmentation of DNA in B16 cells (E).
323 Representative images of the melanoma cell line B16 upon 1267 nm illumination, upon 1122 nm

illumination and control cells by using NucView 488 and Hoechst 33342 (F). Results of statistical processing of cell death (N=11 (11764 cells) for 1267 nm, N=12 (13885 cells) for 1122 nm, N=10 (15170 cells) for control cells) (G). Representative confocal images of fibroblasts upon 1267 nm illumination and control fibroblasts by using NucView 488 and Hoechst 33342 (H). Results of statistical processing of cell death (N=4 (945 cells) for 1267 nm, N=3 (885 cells) for control cells) (I). *$p < 0.001$

DISCUSSION

Here we show that 1267 nm laser specifically induces generation of singlet oxygen in solution and inside of the fibroblasts and melanoma cells. Although SOSG has a number of disadvantages including slow permeability of this indicator through biological membranes [30], in our experiments, SOSG fluorescence was high enough to detect significant changes in both types of cells (Figure 1). Importantly, other indicators for ROS, which are partially more specific for hydrogen peroxide or superoxide anion show no effect of 1267 nm laser on the production of these, and possibly other types of ROS. Mitochondria are sensitive to any changes in the metabolism or oxygen level that change ROS production [23], however, 1267 nm laser did not change the rate of ROS production in mitochondrial matrix in our experiments. This all helps us to conclude that at 200 J/cm^2, 1267 nm laser only generates singlet oxygen in fibroblasts and melanoma cells.

It is also important to note here that the conducted computer simulation demonstrated the absence of significant heating of the cell culture media for the selected radiation power [31].

Singlet oxygen production did not change the level of major markers of oxidative stress – GSH and lipid peroxidation [26] that suggests absence of the global oxidation in fibroblasts and melanoma cells. More specifically, 1267 nm laser and singlet oxygen should not induce ferroptosis because of absence of effect on lipid peroxidation. Although, activation of ferroptosis by singlet oxygen was recently shown for hepatoma Hepa 1-6 [32], in our experiments 1267 nm laser did not induce lipid

peroxidation and disruption of plasma membrane in experiments with PI that may be due to the different doses of singlet oxygen rather than cell specificity.

Although singlet oxygen did not produce oxidative damage, laser 1267 nm induced apoptotic cell death in melanoma cells but not in fibroblasts. Previously, higher cytotoxicity of PDT-induced singlet oxygen to melanoma cells comparing to fibroblasts was demonstrated without explanation of this specificity [33]. Specificity of singlet oxygen production and triggering apoptosis in cancer cell line without significant oxidative damage suggests fine mechanism of the cell death trigger in melanoma cells. The mechanism of different sensitivity of mitochondrial permeability transition of fibroblasts and B16 melanoma cells to singlet oxygen could be explained by number of factors. The absence of effect of singlet oxygen on PTP in fibroblasts is in agreement with previously shown results that singlet oxygen did not induce any sudden and transient loss of mitochondrial membrane potential in primary neurons and astrocytes [10] and that it inactivated calcium and oxidation-induced mitochondrial permeability transition pore in rat liver mitochondria [34]. However, in isolated mitochondria, PTP can be activated by oxidation of thiols by various ROS in mitochondrial domains containing hematoporphyrin-near, pore-regulating histidines [35]. In live cells, it can be achieved by illumination of the mitochondrial indicators with high laser [36]. However, in our experiments this effect can be excluded because both cell types were illuminated by lasers (including LSM laser) in similar conditions, but it induced PTP opening only in cancer cell line. It suggests specific vulnerability of melanoma cells to oxidation of thiols in the mechanisms of PTP opening, that triggers apoptotic cascade and leads to cell death.

However, we singlet oxygen can have more complex effect in the time of induction of apoptosis. Thus, extracellular singlet oxygen production also shown to be able to induce tumor cell-specific apoptosis-inducing ROS signaling [37]. Such specific vulnerability of melanoma cancer cell line to singlet oxygen comparing to control fibroblasts may be used as potential treatment in some cancers.

COMPETING INTEREST

The authors declare that they have no known competing financial interests or personal relationships that could have appeared to influence the work reported in this paper.

ACKNOWLEDGEMENTS

This work was supported by the grant of the Russian Federation Government no. 075-15-2019-1877. The work was also supported by the grant of the President of the Russian Federation for state support of young Russian scientists No. MK-398.2021.4 (development of experimental setup and data acquisition).

REFERENCES

[1] W.A. Pryor, K.N. Houk, C.S. Foote, J.M. Fukuto, L.J. Ignarro, G.L. Squadrito, K.J.A. Davies, Free radical biology and medicine: It's a gas, man!, Am. J. Physiol. - Regul. Integr. Comp. Physiol. 291 (2006) R491-511. https://doi.org/10.1152/ajpregu.00614.2005.

[2] S. Gandhi, A.Y. Abramov, Mechanism of oxidative stress in neurodegeneration, Oxid. Med. Cell. Longev. 2012 (2012). https://doi.org/10.1155/2012/428010.

[3] J.M.C. Gutteridge, B. Halliwell, Mini-review: oxidative stress, redox stress or redox success?, Biochem. Biophys. Res. Commun. 502 (2018) 183–186. https://doi.org/10.1016/j.bbrc.2018.05.045.

[4] W. Dröge, Free radicals in the physiological control of cell function, Physiol. Rev. 82 (2002) 47–95. https://doi.org/10.1152/physrev.00018.2001.

[5] L. Zhang, X. Wang, R. Cueto, C. Effi, Y. Zhang, H. Tan, X. Qin, Y. Ji, X. Yang, H. Wang, Biochemical basis and metabolic interplay of redox regulation, Redox Biol. 26 (2019). https://doi.org/10.1016/j.redox.2019.101284.

[6] I.N. Novikova, A. Manole, E.A. Zherebtsov, D.D. Stavtsev, M.N. Vukolova, A. V. Dunaev, P.R. Angelova, A.Y. Abramov, Adrenaline induces calcium signal in astrocytes and vasoconstriction via activation of monoamine oxidase, Free Radic. Biol. Med. 159 (2020) 15–22. https://doi.org/10.1016/j.freeradbiomed.2020.07.011.

[7] M. V. Avshalumov, L. Bao, J.C. Patel, M.E. Rice, H2O2 signaling in the nigrostriatal dopamine pathway via ATP-sensitive potassium channels: Issues and answers, Antioxidants Redox Signal. 9 (2007) 219–231. https://doi.org/10.1089/ars.2007.9.219.

[8] S.W. Ryter, R.M. Tyrrell, Singlet molecular oxygen (1O2): A possible effector of eukaryotic

gene expression, Free Radic. Biol. Med. 24 (1998) 1520–1534. https://doi.org/10.1016/S0891-5849(97)00461-9.

[9] S. Zhuang, J.T. Demirs, I.E. Kochevar, Protein kinase C inhibits singlet oxygen-induced apoptosis by decreasing caspase-8 activation, Oncogene. 20 (2001) 6764–6776. https://doi.org/10.1038/sj.onc.1204867.

[10] S.G. Sokolovski, E.U. Rafailov, A.Y. Abramov, P.R. Angelova, Singlet oxygen stimulates mitochondrial bioenergetics in brain cells, Free Radic. Biol. Med. 163 (2021) 306–313. https://doi.org/10.1016/j.freeradbiomed.2020.12.022.

[11] M. Westberg, M. Bregnhøj, A. Blázquez-Castro, T. Breitenbach, M. Etzerodt, P.R. Ogilby, Control of singlet oxygen production in experiments performed on single mammalian cells, J. Photochem. Photobiol. A Chem. 321 (2016) 297–308. https://doi.org/10.1016/j.jphotochem.2016.01.028.

[12] S.G. Sokolovski, S.A. Zolotovskaya, A. Goltsov, C. Pourreyron, A.P. South, E.U. Rafailov, Infrared laser pulse triggers increased singlet oxygen production in tumour cells, Sci. Rep. 3 (2013) 1–7. https://doi.org/10.1038/srep03484.

[13] B.C. Wilson, M.S. Patterson, The physics, biophysics and technology of photodynamic therapy, Phys. Med. Biol. 53 (2008). https://doi.org/10.1088/0031-9155/53/9/R01.

[14] F. Anquez, A. Sivéry, I. El Yazidi-Belkoura, J. Zemmouri, P. Suret, S. Randoux, E. Courtade, Chapter 4. Production of Singlet Oxygen by Direct Photoactivation of Molecular Oxygen, in: 2016: pp. 75–91. https://doi.org/10.1039/9781782622208-00075.

[15] A. Blázquez-Castro, Direct 1O2 optical excitation: A tool for redox biology, Redox Biol. 13 (2017) 39–59. https://doi.org/10.1016/j.redox.2017.05.011.

[16] S.D. Zakharov, A. V Ivanov, Light-oxygen effect in cells and its potential applications in tumour therapy (review), Quantum Electron. 29 (1999) 1031–1053. https://doi.org/10.1070/qe1999v029n12abeh001629.

[17] F. Anquez, I. El Yazidi-Belkoura, S. Randoux, P. Suret, E. Courtade, Cancerous cell death from sensitizer free photoactivation of singlet oxygen, Photochem. Photobiol. 88 (2012) 167–174. https://doi.org/10.1111/j.1751-1097.2011.01028.x.

[18] Y. V. Saenko, E.S. Glushchenko, I.O. Zolotovskii, E. Sholokhov, A. Kurkov, Mitochondrial dependent oxidative stress in cell culture induced by laser radiation at 1265 nm, Lasers Med. Sci. 31 (2016) 405–413. https://doi.org/10.1007/s10103-015-1861-z.

[19] N.R. Komilova, P.R. Angelova, A. V Berezhnov, O.A. Stelmashchuk, U.Z. Mirkhodjaev, H. Houlden, A. V Gourine, N. Esteras, A.Y. Abramov, Metabolically induced intracellular pH changes activate mitophagy, autophagy, and cell protection in familial forms of Parkinson's disease, FEBS J. 289 (2022) 699–711.

[20] H. Zhao, S. Kalivendi, H. Zhang, J. Joseph, K. Nithipatikom, J. Vásquez-Vivar, B. Kalyanaraman, Superoxide reacts with hydroethidine but forms a fluorescent product that is distinctly different from ethidium: potential implications in intracellular fluorescence detection of superoxide, Free Radic. Biol. Med. 34 (2003) 1359–1368. https://doi.org/10.1016/s0891-5849(03)00142-4.

[21] R. Michalski, B. Michalowski, A. Sikora, J. Zielonka, B. Kalyanaraman, On the use of fluorescence lifetime imaging and dihydroethidium to detect superoxide in intact animals and ex vivo tissues: a reassessment, Free Radic. Biol. Med. 67 (2014) 278–284. https://doi.org/10.1016/j.freeradbiomed.2013.10.816.

[22] S.L. Hempel, G.R. Buettner, Y.Q. O'Malley, D.A. Wessels, D.M. Flaherty, Dihydrofluorescein diacetate is superior for detecting intracellular oxidants: comparison with 2′, 7′-dichlorodihydrofluorescein diacetate, 5 (and 6)-carboxy-2′, 7′-dichlorodihydrofluorescein diacetate, and dihydrorhodamine 123, Free Radic. Biol. Med. 27 (1999) 146–159.

[23] P.R. Angelova, A.Y. Abramov, Functional role of mitochondrial reactive oxygen species in physiology, Free Radic. Biol. Med. 100 (2016) 81–85. https://doi.org/10.1016/j.freeradbiomed.2016.06.005.

[24] G. Manda, M.E. Hinescu, I. V Neagoe, L.F. V Ferreira, R. Boscencu, P. Vasos, S.H. Basaga, A. Cuadrado, Emerging therapeutic targets in oncologic photodynamic therapy, Curr Pharm Des. 24 (2018) 5268–5295. https://doi.org/10.2174/1381612825666190122163832.

[25] A.-M. Domijan, S. Kovac, A.Y. Abramov, Lipid peroxidation is essential for phospholipase C activity and the inositol-trisphosphate-related Ca2+ signal, J. Cell Sci. 127 (2014) 21–26. https://doi.org/10.1242/jcs.138370.

[26] P.R. Angelova, N. Esteras, A.Y. Abramov, Mitochondria and lipid peroxidation in the mechanism of neurodegeneration: finding ways for prevention, Med. Res. Rev. 41 (2021) 770–784. https://doi.org/10.1002/med.21712.

[27] A.Y. Abramov, P.R. Angelova, Cellular mechanisms of complex I-associated pathology, Biochem. Soc. Trans. 47 (2019) 1963–1969. https://doi.org/10.1042/BST20191042.

[28] P. Bernardi, F. Di Lisa, F. Fogolari, G. Lippe, From ATP to PTP and back: a dual function for the mitochondrial ATP synthase, Circ. Res. 116 (2015) 1850–1862. https://doi.org/10.1161/CIRCRESAHA.115.306557.

[29] H. Cen, F. Mao, I. Aronchik, R.J. Fuentes, G.L. Firestone, DEVD-NucView488: A novel class of enzyme substrates for real-time detection of caspase-3 activity in live cells, FASEB J. 22 (2008) 2243–2252.

[30] S. Kim, M. Fujitsuka, T. Majima, Photochemistry of singlet oxygen sensor green, J. Phys.

Chem. B. 117 (2013) 13985–13992. https://doi.org/10.1021/jp406638g.

[31] V. Dremin, I. Novikova, E. Rafailov, Simulation of thermal field distribution in biological tissue and cell culture media irradiated with infrared wavelengths, Opt. Express. (2022).

[32] T. Homma, S. Kobayashi, J. Fujii, Induction of ferroptosis by singlet oxygen generated from naphthalene endoperoxide, Biochem. Biophys. Res. Commun. 518 (2019) 519–525. https://doi.org/10.1016/j.bbrc.2019.08.073.

[33] K. Khorsandi, R. Hosseinzadeh, E. Chamani, Molecular interaction and cellular studies on combination photodynamic therapy with rutoside for melanoma A375 cancer cells: an in vitro study, Cancer Cell Int. 20 (2020) 1–15. https://doi.org/10.1186/s12935-020-01616-x.

[34] C. Salet, G. Moreno, F. Ricchelli, P. Bernardi, Singlet oxygen produced by photodynamic action causes inactivation of the mitochondrial permeability transition pore, J. Biol. Chem. 272 (1997) 21938–21943.

[35] F. Ricchelli, J. Šileikytė, P. Bernardi, Shedding light on the mitochondrial permeability transition, Biochim. Biophys. Acta (BBA)-Bioenergetics. 1807 (2011) 482–490.

[36] M.H.R. Ludtmann, P.R. Angelova, M.H. Horrocks, M.L. Choi, M. Rodrigues, A.Y. Baev, A. V Berezhnov, Z. Yao, D. Little, B. Banushi, α-synuclein oligomers interact with ATP synthase and open the permeability transition pore in Parkinson's disease, Nat. Commun. 9 (2018) 1–16. https://doi.org/10.1038/s41467-018-04422-2.

[37] M. Riethmüller, N. Burger, G. Bauer, Singlet oxygen treatment of tumor cells triggers extracellular singlet oxygen generation, catalase inactivation and reactivation of intercellular apoptosis-inducing signaling, Redox Biol. 6 (2015) 157–168.

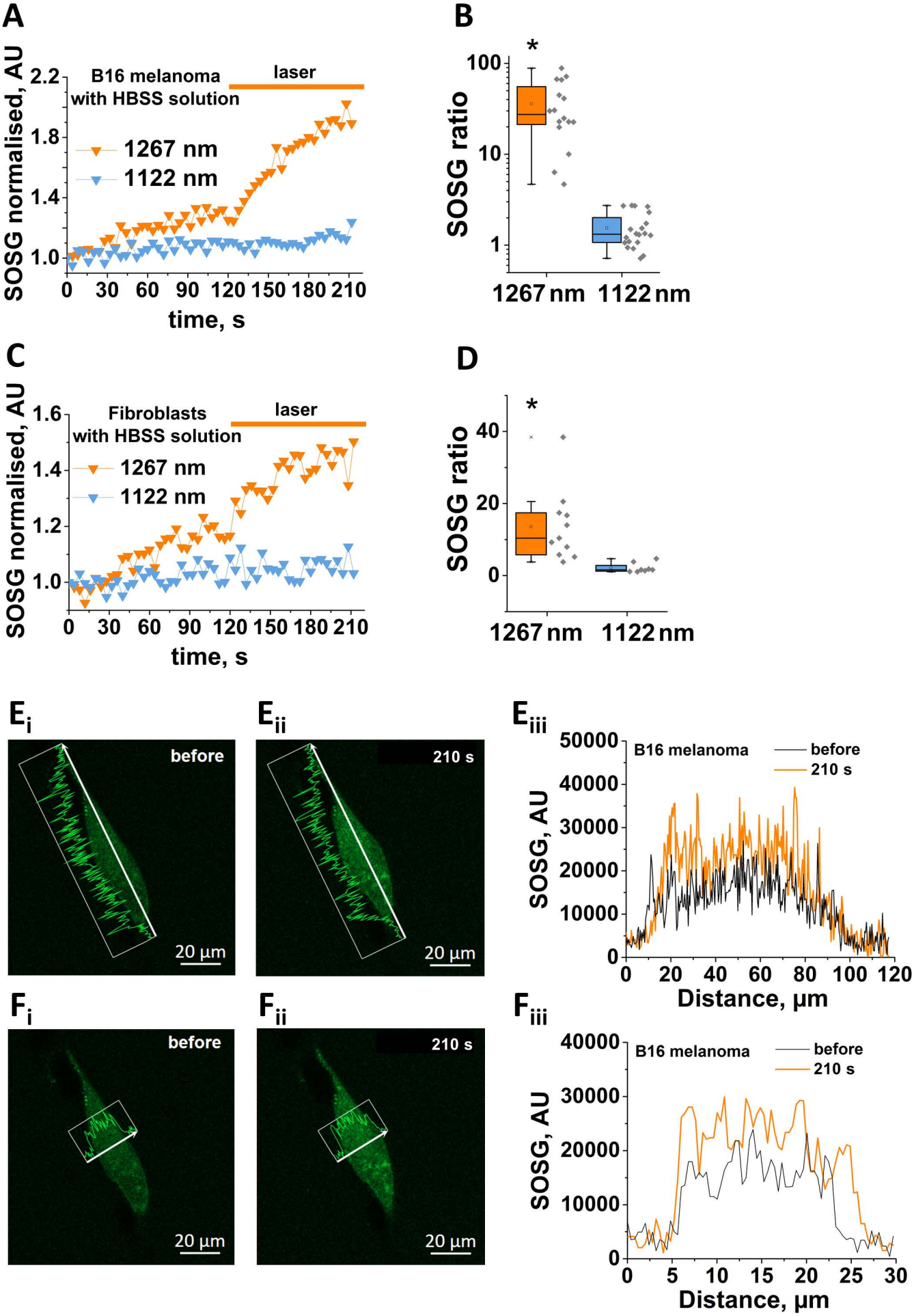
A
B16 melanoma
with HBSS solution
laser
1267 nm
1122 nm
SOSG normalised, AU
time, s
B
SOSG ratio
1267 nm
1122 nm
C
Fibroblasts
with HBSS solution
laser
1267 nm
1122 nm
SOSG normalised, AU
time, s
D
SOSG ratio
1267 nm
1122 nm
Ei
before
20 µm
Eii
210 s
20 µm
Eiii
B16 melanoma
before
210 s
SOSG, AU
Distance, µm
Fi
before
20 µm
Fii
210 s
20 µm
Fiii
B16 melanoma
before
210 s
SOSG, AU
Distance, µm

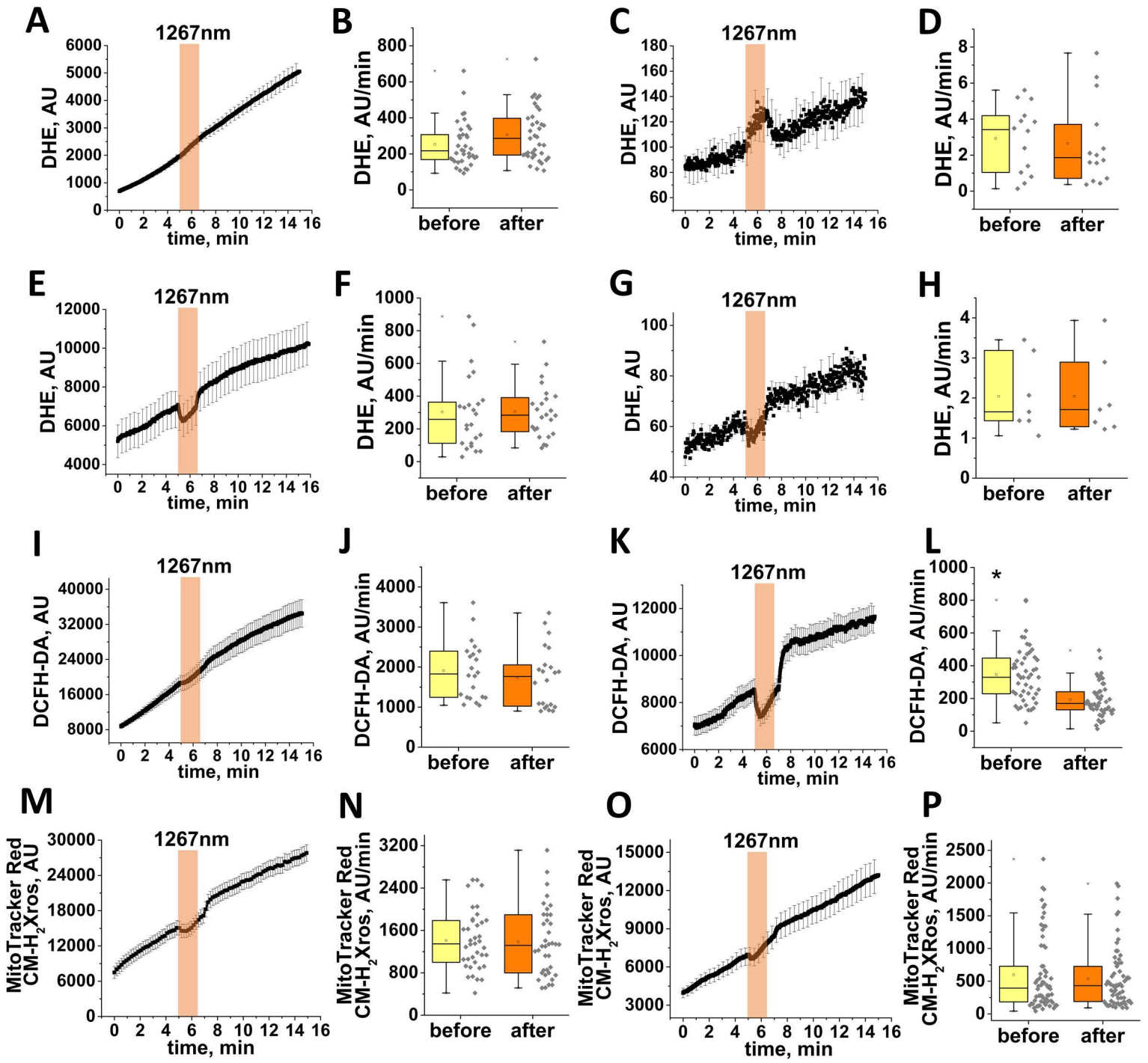
A
1267nm
DHE, AU
time, min
B
DHE, AU/min
before
after
C
1267nm
DHE, AU
time, min
D
DHE, AU/min
before
after
E
1267nm
DHE, AU
time, min
F
DHE, AU/min
before
after
G
1267nm
DHE, AU
time, min
H
DHE, AU/min
before
after
I
1267nm
DCFH-DA, AU
time, min
J
DCFH-DA, AU/min
before
after
K
1267nm
DCFH-DA, AU
time, min
L
*
DCFH-DA, AU/min
before
after
M
1267nm
MitoTracker Red CM-H2Xros, AU
time, min
N
MitoTracker Red CM-H2Xros, AU/min
before
after
O
1267nm
MitoTracker Red CM-H2Xros, AU
time, min
P
MitoTracker Red CM-H2XRos, AU/min
before
after

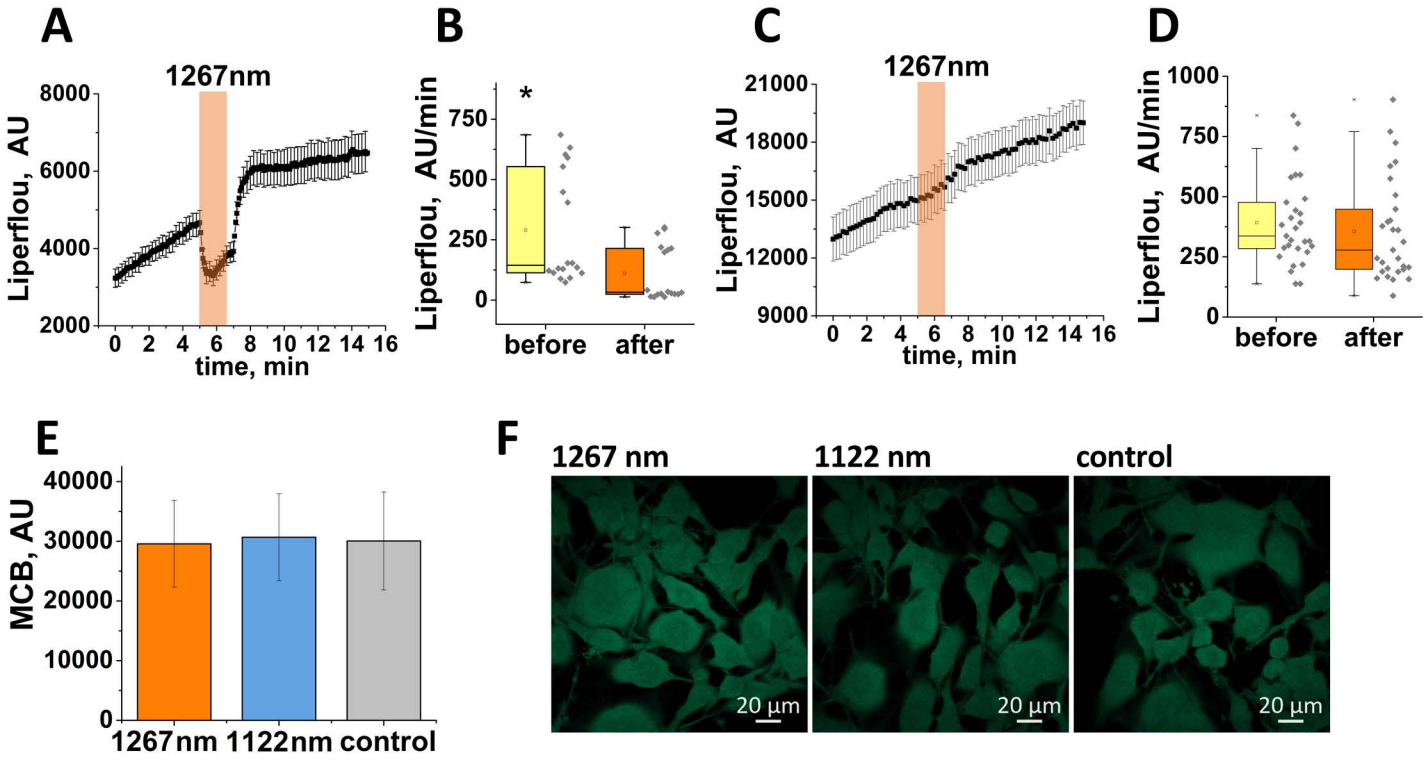
A
1267nm
Liperflou, AU
8000
6000
4000
2000
0 2 4 6 8 10 12 14 16
time, min
B
*
Liperflou, AU/min
750
500
250
0
before
after
C
1267nm
Liperflou, AU
21000
18000
15000
12000
9000
0 2 4 6 8 10 12 14 16
time, min
D
Liperflou, AU/min
1000
750
500
250
0
before
after
E
MCB, AU
40000
30000
20000
10000
0
1267nm 1122nm control
F
1267 nm
1122 nm
control
20 µm
20 µm
20 µm

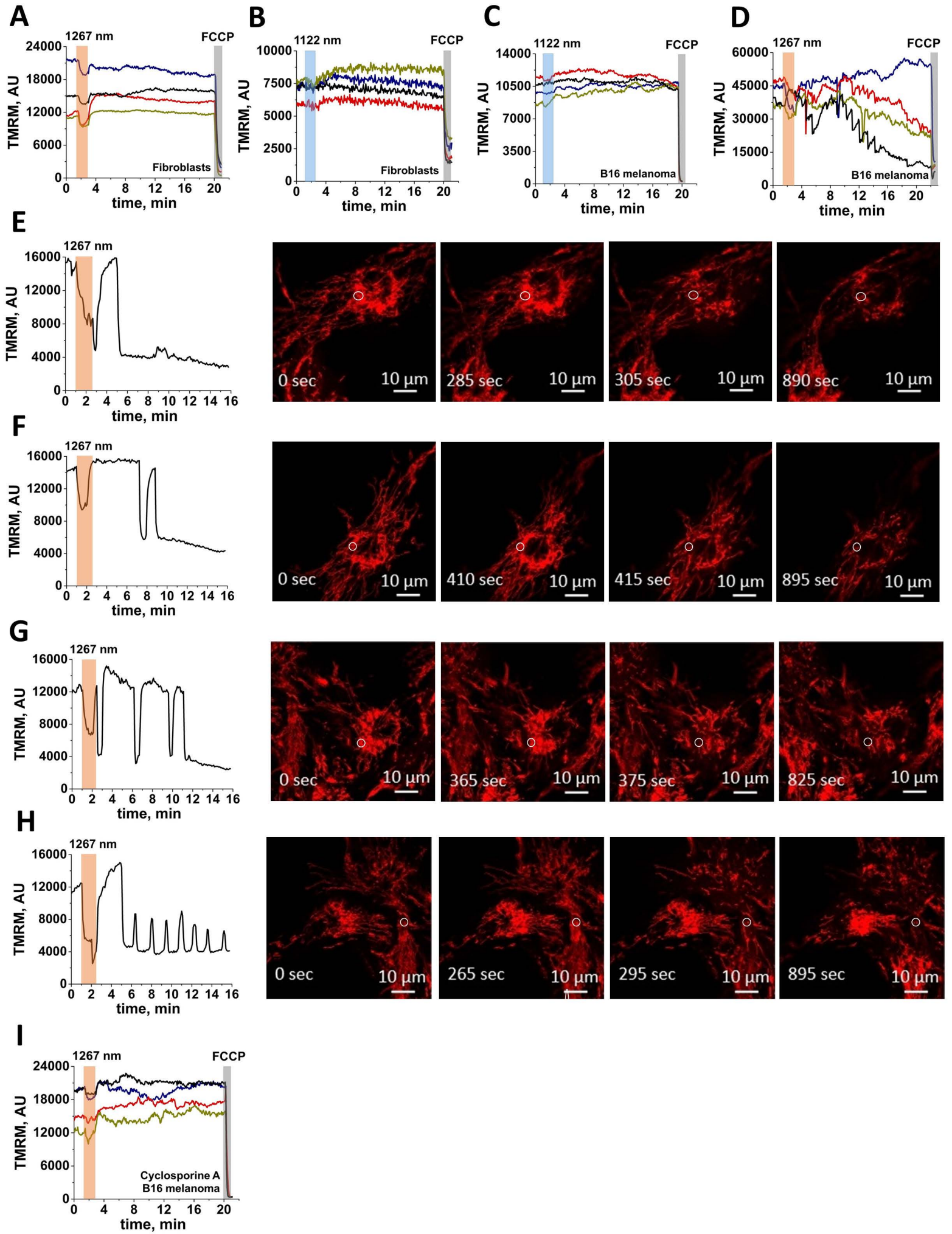
A
1267 nm
FCCP
TMRM, AU
Fibroblasts
time, min
B
1122 nm
FCCP
TMRM, AU
Fibroblasts
time, min
C
1122 nm
FCCP
TMRM, AU
B16 melanoma
time, min
D
1267 nm
FCCP
TMRM, AU
B16 melanoma
time, min
E
1267 nm
TMRM, AU
time, min
0 sec
285 sec
305 sec
890 sec
10 µm
F
1267 nm
TMRM, AU
time, min
0 sec
410 sec
415 sec
895 sec
10 µm
G
1267 nm
TMRM, AU
time, min
0 sec
365 sec
375 sec
825 sec
10 µm
H
1267 nm
TMRM, AU
time, min
0 sec
265 sec
295 sec
895 sec
10 µm
I
1267 nm
FCCP
TMRM, AU
Cyclosporine A
B16 melanoma
time, min

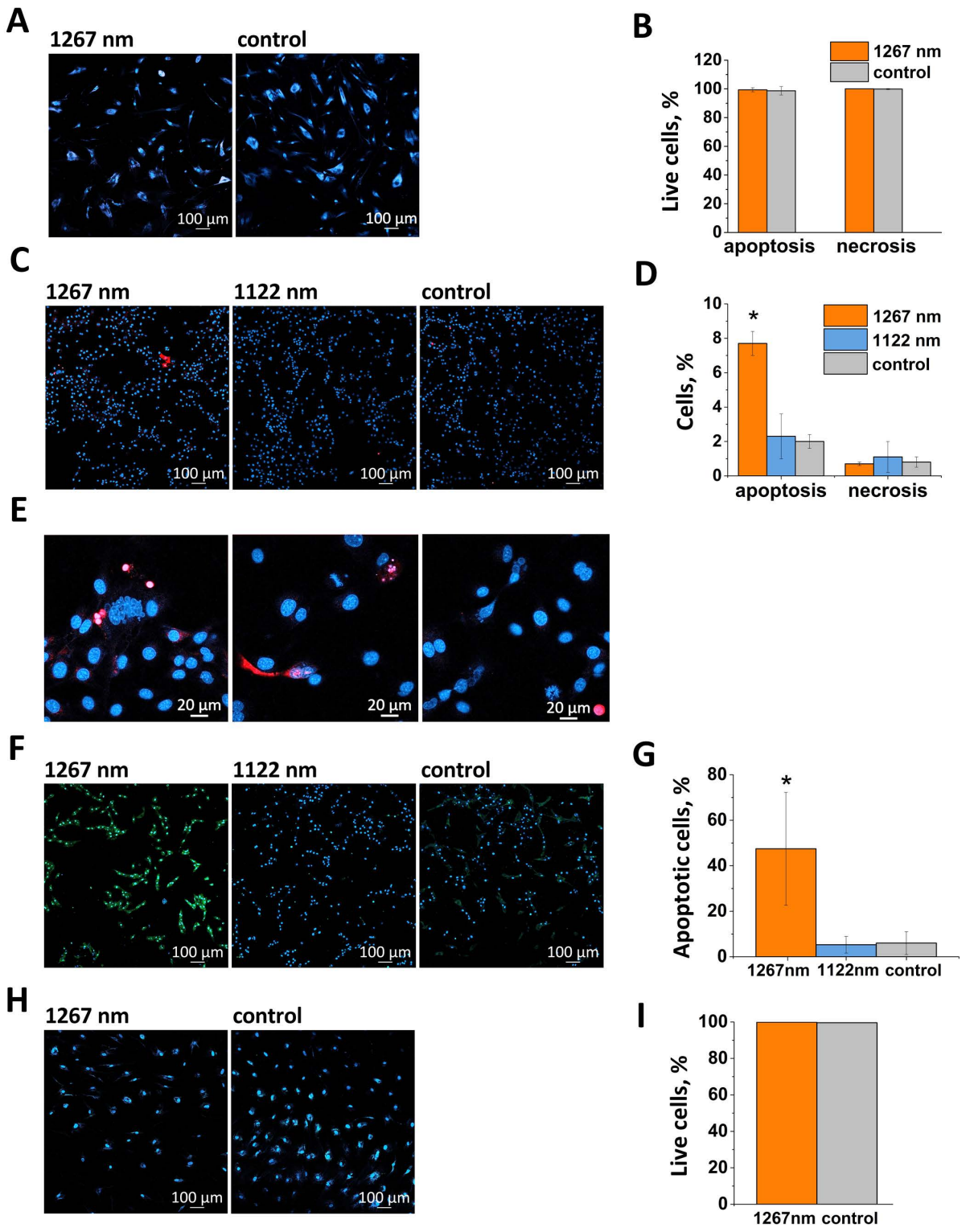
A
1267 nm
control
100 μm
100 μm
B
1267 nm
control
Live cells, %
120
100
80
60
40
20
0
apoptosis
necrosis
C
1267 nm
1122 nm
control
100 μm
100 μm
100 μm
D
1267 nm
1122 nm
control
Cells, %
10
8
6
4
2
0
*
apoptosis
necrosis
E
20 μm
20 μm
20 μm
F
1267 nm
1122 nm
control
100 μm
100 μm
100 μm
G
Apoptotic cells, %
80
60
40
20
0
*
1267nm
1122nm
control
H
1267 nm
control
100 μm
100 μm
I
Live cells, %
100
80
60
40
20
0
1267nm
control